06

# Deformation component of electrical resistance of thin tungsten samples at high shock-pressures loading

© A.M. Molodets, A.A. Golyshev, V.V. Kim

Federal Research Center of Problems of Chemical Physics and Medicinal Chemistry of RAS,
142432 Chernogolovka, Moscow region, Russia
e-mail: molodets@icp.ac.ru

*Received 2025*
*Revised 2025*
*Accepted 2025*

The electrical resistance of tungsten samples was measured under shock wave loading up to 15 GPa. The experiment was analyzed and modeled taking into account the volume-temperature and deformation components of the electrical resistance of tungsten. The relationship between the excessive electrical resistance of the deformation component and the characteristics of the absolute deformation rate of tungsten under planar one-dimensional loading is considered.

**Keywords:** electrical resistance, tungsten, equations of state, shock waves, deformation, strain rate, hydrocode.

DOI: 10.61011/TP.2026.04.63268.266-25

## Introduction

As known, measurement of electrical resistance of shock-compressed materials is widely used in studies of various processes and effects that accompany shock-wave loading of condensed media. In relation to metals, these effects include polymorphous transformations, a transition metal–dielectric and dielectric–metal, volume-temperature dependences of conductivity, etc. (see [1–3] and the bibliography therein).

Electrical resistance of shock-compressed metals is usually measured under planar one-dimensional loading conditions using thin foil samples that are arranged parallel to a shock-wave front. The metal samples are placed between layers of an insulator, whose stiffness is as a rule different from stiffness of the metal under study. In a situation when a sample thickness turns out to be much smaller than the insulator thickness, and stiffness, on the contrary, significantly exceeds stiffness of the insulator a sample loading history has a cyclic component that is caused by reverberation of compression and unloading waves in the sample (see [1,4]). If, additionally, amplitudes of shock waves significantly exceed yield strength of the metal under study, then at a cyclic loading stage the sample is subjected to high-rate plastic deformation that stimulates defect formation in the metal and irreversibly increases electrical resistance of the metal sample thereby. Thus, in addition to a reversible volume-temperature component, measurement of electrical resistance of the shock-compressed thin metal samples around the soft insulator can also have an irreversible deformation component of electrical resistance, which is caused by defect formation during high-rate plastic deformation.

The effect and value of the deformation component of electrical resistance of the metals have been experimentally studied directly during their shock-wave loading since the 1980s (see [5] and the bibliography therein). But it should be noted that experimental values of electrical resistance are analyzed in these studies based on their baric dependence. It seems that in a logic of the above-described diagram of origination of the deformation component of electrical resistance, it is more preferable to rely on a dependence of excessive electrical resistance on deformation, rather than pressure. In this context, the present study was aimed at finding a relation between excessive electrical resistance of the thin tungsten samples and characteristics of their deformation during flat one-dimensional loading.

Tungsten was selected to be a model material due to its low compressibility that minimizes heating and, therefore, defect annealing during shock compression as well as due to the fact that a rheological behavior of tungsten under flat one-dimensional loads can be with satisfactory accuracy represented by an ideal elastic-plastic model (see [6] and the bibliography therein).

## 1. Samples and the measuring cell

The samples for shock-wave studies were manufactured from a VA-grade tungsten foil of the thickness of 0.05 mm. According to the specification TU 48-19-188-91, a chemical composition of this foil in wt.Al $\leq 0.002$ %, Fe $\leq 0.009$ %, Ni $\leq 0.004$ %, Ca $\leq 0.010$ %, Si $\leq 0.004$ %, Mo $\leq 0.40$ %. A tape sample *1* was mechanically cut out of the foil sheet (Fig. 1). A signal wire and an earthing braid of the RK-75 high-frequency cable were soldered to sample's copper-plated ends *2*. A thickness of the tungsten samples was $h_0 = 0.050(1)$ mm, and their width was $a_0 \approx 1-4.0$ mm.

A plane of the tape sample was parallel to a shock wave front plane. The same plane included the measuring cell of the manganin gauger *3, 4*, i.e. the cell of the manganin gauger was actually analogous to the measuring cell of the

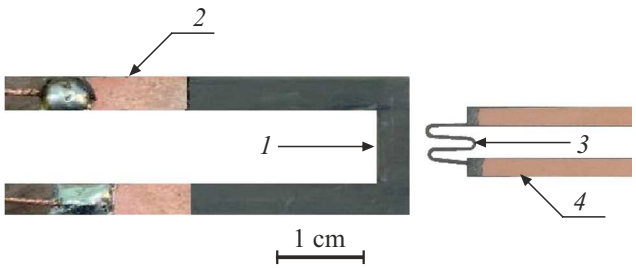


**Figure 1.** Measuring cell. *1* — the Π-shaped tungsten sample of the thickness $h_0 = 0.052$ mm, *2* — the copper-plated current conductors, *3* — the sensitive element of a manganin pressure gauger, which has a thickness of 0.035 mm, *4* — the copper current conductors of the thickness of 0.015 mm.

sample, in which the tungsten sample is replaced by the manganin tape sample.

Initial electrical resistances$R_0$ of the tungsten and manganin samples were measured preliminarily for each experiment and were $R_0 \approx 0.025(1)\,\Omega$ for tungsten and $\approx 1.5\,\Omega$ for manganin.

## 2. Generator of stage-cyclic shock-wave loading and conserving of the samples

The present study has used a generator of stage-cyclic shock-wave loading, which is schematically shown in Fig. 2, *a*. Operation of this generator is described in detail in [4,7]. In short, it is as follows. A metal flat impactor *1* is accelerated by an explosion device to the velocity $W_0$. As a result of collision of the impactor *1* with a target *2*–*4* a teflon insulator *3* is stagedly shock-compressed to gigapascal pressures. The insulator *3* included the manganin pressure gauger *5*. The same plane also includes the tungsten tape sample *6*. Alternate arrival of each compression state to the gauger *5* and the sample *6* is accompanied by synchronous reverberation of evanescent waves of compression and unloading in them. Since the sample thicknesses are selected to be much smaller than the insulator thickness and stiffness of the metals significantly exceeds stiffness of PTFE, then the front of each stage of shock compression contains a high-frequency cyclic component that is caused by reverberation of the compression and unloading waves in the sample. After arrival of the unloading waves from a rear side of the impactor *1* or from a free surface of a plate *4* pressure in the gauger *5* and the sample *6* synchronously decreases to zero values.

This generator was used in an identical separate test of sample conservation. In this experiment, the manganin gauger near the Π-shaped sample was replaced by tungsten foil strips cut out of adjacent portions of the Π-sample (Fig. 2, *b*). The manufactured identical analogue of a lamellar target *2*–*6* (Fig. 2, *a*) was fastened by four metal bolts and placed to a thick (50 mm) iron plate.

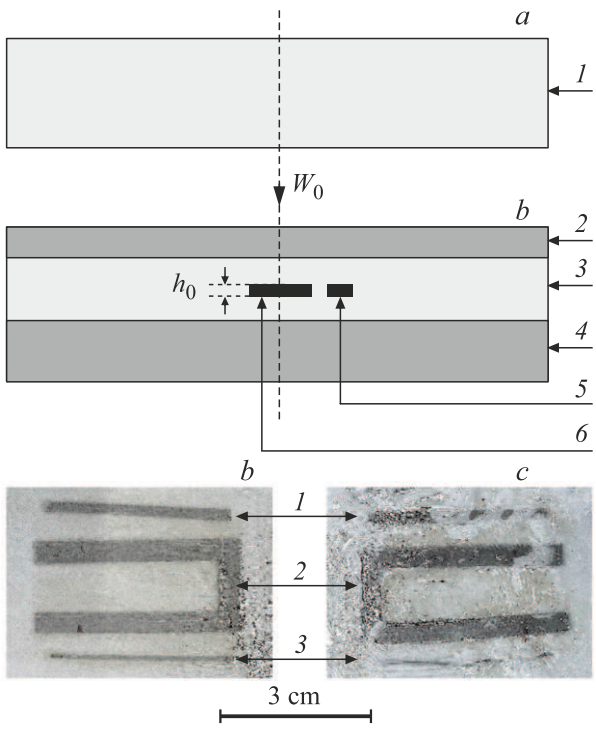


**Figure 2.** Generator of stage-cyclic shock-wave loading. *a* — *1* — the aluminum impactor of the thickness of 7.0 mm with the velocity $W_0 = 1.05$ km/s, *2* — the steel (the 18-8 steel) plate of the thickness of 1.97 mm, *3* — the set of PTFE films with the total thickness of 1.22 mm, *4* — the steel plate of the thickness of 3.77 mm, *5* — the manganin pressure gauger, *6* — the tungsten sample; *b* — the tungsten foil samples before loading; *c* — the samples subjected to staged-cyclic shock-wave loading; *1, 3* — the tungsten strips of the thickness of 0.05 mm, *2* — the copy of the tungsten Π-sample of the thickness of 0.05 mm.

The tungsten strips *1, 3* and the Π-sample *2* before loading (Fig. 2, *b*) and after explosion loading, conservation and disassembly of the lamellar target are shown in Fig. 2, *c*. Sizes and electrical resistances of the conserved samples were measured for subsequent comparison with their values before explosion loading. The results were as follows. Changes of the linear sizes, i.e. deformations in the shock wave plane, did not exceed 1 %. Changes of the thicknesses, i.e. along propagation of the shock wave, did not exceed 1 % as well. Electrical resistance along the $R_{sh}$ strips exceeded by no more than 5(3) %, i.e. $R_{sh} \leq 1.05(3)R_0$. An error was a deviation from the arithmetic mean.

## 3. Electrical resistance profiles of the shock-compressed tungsten samples

Electrical resistance of the sample and manganin was measured in a two-point scheme with the Wheatstone bridge containing the corresponding measuring cell (see Fig. 1) as the resistance to be measured. During the explosion experiment, direct currents $J_0 = 3.0(1)$ A were transmitted

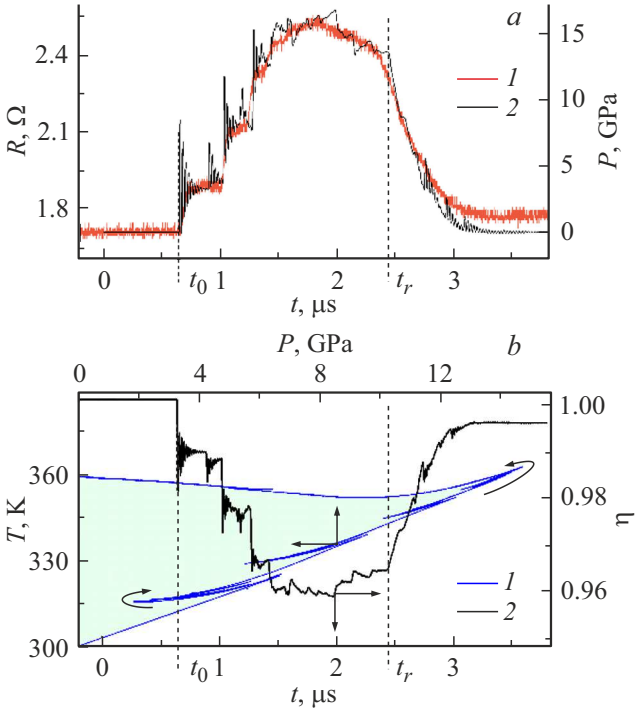


**Figure 3.** History (the dependence on time $t$) of the volume-temperature state of the metal samples under conditions of stage-cyclic shock compression and subsequent unloading. *a* — *1* — the experimental record of the electrical resistance $R$ of the manganin gauger under staged shock compression and unloading, *2* — the model profile of pressure $P$ in the tungsten sample, $t_0$ — the moment of arrival of the first shock wave, $t_r$ — the moment of arrival of the first characteristic of the unloading wave; *b* — *1* — history of the thermodynamic state of tungsten in the coordinates pressure ($P$) — temperature ($T$) under compression and unloading (the round arrows mark a sequence of the $PT-$states in time), *2* — the relative change of the thickness $\eta = h/h_0$, $h$ — the current value of the thickness of tungsten sample, $h_0$ — the initial thickness of the sample.

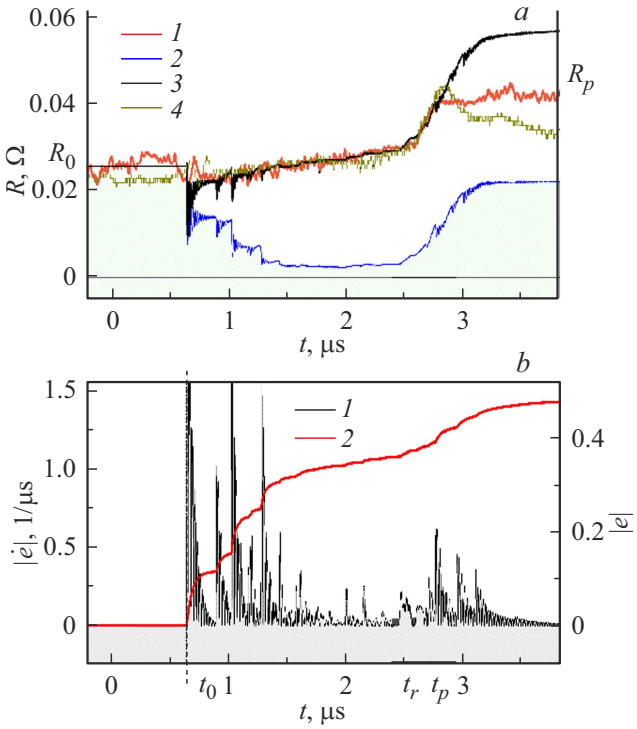


**Figure 4.** Volume-temperature and deformation components of electrical resistance of the thin tungsten sample under staged-cyclic shock compression. *a* — *1* — the experimental profile $R = R(t)$ of electrical resistance of the tungsten sample, which is measured in a two-point scheme, *2* — the model profile of the volume-temperature component of electrical resistance $R_1 = R_1(t)$ (5), *3* — the summed model profile $R_{mod} = R_{mod}(t)$ of electrical resistance of the tungsten sample (7), *4* — the profile of electrical resistance of the tungsten tape sample, which is measured in a four-point scheme; *b* — *1* — the absolute value of the strain rate of the sample, *2* — the time integral of the absolute value of the strain rate of the sample; $t_0$ and $t_r$ are the same as in Fig. 3, $t_p$ — the moment of sharp dissonance of the model and the experiment.

from independent current sources along the tungsten and manganin tape samples. Profiles (dependences on time $t$) of variation of bridge disbalance voltage $\Delta U = \Delta U(t)$ were measured and they were recorded by the Tektronix DPO4104B high-frequency oscilloscope. The profiles $\Delta U(t)$ were recalculated into changes of electrical resistance by the formula $\Delta R = k\Delta U$, where $k$ is a pre-determined calibration coefficient. The experimental profile of electrical resistance of the sample $R = R(t)$ was calculated as $R = R_0 + \Delta R$, where $R_0$ is its initial electrical resistance. Results of an optimal experiment are provided as profiles of electrical resistances of the manganin sample *1* in Fig. 3, *a* and a profile of the tungsten sample *1* in Fig. 4, *a*.

Besides, a separate experiment with the same setup was taken to measure the profile of electrical resistance of the tungsten tape sample in the four-point scheme that excluded electrical resistance of current conductors. This profile is designated by the digit *4* in Fig. 4, *a*.

## 4. Modeling of electrical resistance of the tungsten samples under high dynamic pressures

It was assumed that the experimental profiles of electrical resistance of the tungsten samples under high dynamic pressures were determined by two components. The first component is caused by a property of the metal in the form of a reversible volume-temperature dependence of specific electrical resistivity of tungsten. The second component (a deformation one) is caused by an increase of electrical resistance due to defect formation during high-rate plastic deformation.

The volume-temperature dependences of specific electrical resistance of tungsten under high dynamic pressures were reconstructed based on literature data under conditions of high hydrostatic pressures and temperatures. Patterns of the deformation components were reconstructed within the framework of a phenomenological model based on the

obtained experimental profiles of electrical resistance of the tungsten samples.

### 4.1. Modeling of the thermodynamic state of tungsten under conditions of stages-cyclic shock-wave loading

The thermodynamic state of tungsten was modelled as included in the experimental diagram in Fig. 2 in a specifically-designed one-dimensional hydrocode, in which input data include thicknesses of plates of the experiment done, their equations of state and the impactor velocity $W_0$. For manganin, the equation of state of this alloy from the study [7] were used. The equation of state of tungsten are taken from the study [8]. The thermal equation of state and its parameters for tungsten are given in Appendix. The hydrocode took into account the rheological behavior of tungsten within the framework of the model of the ideal elastic-plastic solid body with parameters from the study [6]. The studied sample was modeled by a plate with an initial thickness $h_0$, since the width of the tungsten tape sample $a_0$ exceeded the value of $h_0$ by orders.

Outcomes of the hydrocode are thermodynamic states of any Lagrangian particle of each plate of the multi-layer target of the explosion generator under flat one-dimensional shock-wave loading. The model results are output as time dependences (profiles) of pressure $P(t)$, the temperature $T(t)$ and the specific volume $V(t)$ for a selected particle. The graph *2* in Fig. 3, *a* shows a model profile pressure $P(t)$ for the tungsten sample of a specific optimal experiment. Exclusion of time from the calculated profiles $P(t)$ and $T(t)$ provides a phase path (a thermodynamic history) $T(P)$ in the coordinates pressure–temperature in each experiment. The graph *1* in Fig. 3, *b* shows the phase path of staged-cyclic compression in the experiment with a specified value $W_0 = 1.05$ km/s.

The value of the velocity $W_0$ of the aluminum impactor in the experiments done by the scheme of Fig. 1 was refined when modeling a specific experiment based on experimental readings of the manganin gauger. For this purpose, electrical resistance of the manganin gauger, for example, the profile *1* in Fig. 3, *a* was traditionally converted (see [7]) into the pressure profile. Then, the hydrocode was used to calculated a series of the model pressure profiles in manganin, which were obtained at several values $W_0 \sim 1.0$ km/s and to select an optimal value of $W_0$, at which the model pressure profile coincided with the experiment. For the experiment considered below, the value of $W_0$ was $W_0 = 1.05(1)$ km/s. This value was used when calculating the phase path *1* in Fig. 3, *b*, which makes it possible to designate an experimentally-studied area of a phase diagram of tungsten to the temperatures of 360 K and pressures of up to 15 GPa.

### 4.2. Modeling of the volume-temperature dependence of specific electrical resistance of tungsten and electrical resistance of the tungsten sample

Similar to [4], the volume ($V$) — temperature ($T$) dependence of specific electrical resistance $\rho = \rho(V, T)$ was modelled as a product of initial specific electrical resistance $\rho_0$ under the normal conditions and two functions: the volume component $\varphi = \varphi(V)$ and the temperature component $\epsilon = \epsilon(T)$.

The value $\rho_0 = 5.28\,\mu\Omega\cdot$cm recommended in the study [9] was taken as initial specific electrical resistance. A power function used in the study [4] was taken as the volume component $\varphi = \varphi(V)$:

$$\varphi = \left(\frac{V}{V_0}\right)^{n/3} \left(\frac{\upsilon_0 - V}{\upsilon_0 - V_0}\right)^{-2n}, \qquad (1)$$

where $\upsilon_0$ is an individual parameter of the metal, $V_0$ is its specific volume at the room temperature $T_0$ and under the atmospheric pressure $P_0$. The parameters $\upsilon_0$ and $V_0$ are known parameters of the equations of state. They are taken for tungsten from the study [8]. The parameter $n$ is a fitting one and can be determined based on experimental data for specific electrical resistance of tungsten at the temperature of 298 K within the pressure range 2–5 GPa, which are taken from the study [10]. For the purposes of the present study, the baric dependence $\rho$ from the study [10] was recalculated into the dependence $\rho = \rho(V)$ by means of the thermal equation of state. These recalculated data are represented by squares *1* in Fig. 5. The value of $n$ was found by a least-square method based on a requirement of the best coincidence of the model graph *1* (Fig. 5) and the experimental array $\rho = \rho(V)$. The value of $n$ and a coefficient of determination $R^2$ turned out to be as follows: $n = 48.5(2.7)$ and $R_2 = 0.97606$. A mutual arrangement of the experiment *1* and the model graph *2* indicates that within the pressure range up to 5 GPa the graph *2* complies with experimental results *1* from the study [10].

For the temperature component of electrical resistance of tungsten, the following empirical power function is taken

$$\epsilon = \rho_0 (T/T_0)^{\alpha}, \qquad (2)$$

where the values $\rho_0 = 5.28\,\mu\Omega\cdot$cm and $T_0 = 293.15$ K are taken according to their values recommended for tungsten under the normal conditions in the study [9]. The value of the fitting parameter $\alpha = 1.2410(5)$ is found using $\rho$ of the array *3* (Fig. 5) of the recommended values of tungsten from the same article [9]. Approximation of an atmospheric isobar of specific electrical resistance of tungsten by the function (2) is designated by the digit *4* in Fig. 5 and provides the values $\alpha = 1.2410(5)$. This value together with the coefficient of determination $R_2 = 0.99992$ is found by the least-square method. As seen, the graph *4* complies with the results [9] within the temperature range 200–450 K.

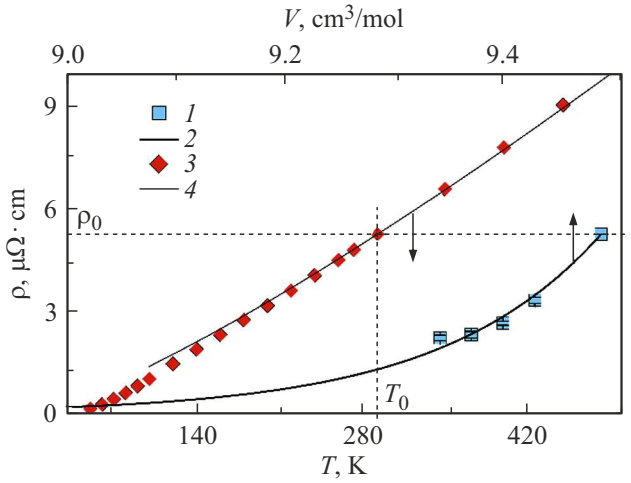


**Figure 5.** Volume ($V$) and temperature ($T$) components of specific electrical resistance $\rho$ of tungsten. *1* — the experimental isotherm $\rho(V)$ up to pressures of 5 GPa at the temperature of 298 K [10], *2* — the graph of the model function (1), including a range of small volumes (high pressures of up to 15 GPa), *3* — the recommended temperature dependence $\rho$ at the atmospheric pressure from the study [9], *4* — the graph of the model function (2).

Thus, taking into account (1) and (2) the model relationship $\rho = \rho(V, T)$ for the volume-temperature dependence of specific electrical resistance of tungsten

$$\rho = \rho_0 \varphi \epsilon \tag{3}$$

complies with the experiment at the pressures below 5 GPa and at temperatures 200–450 K. A set of the parameters (3) for the volume-temperature dependence of electrical resistance of tungsten is shown in Table 1.

We note that based on (3) the expression for the volume-temperature component of electrical resistance of the shock-compressed sample under the conditions of flat one-dimensional compression can be formulated as

$$R = \left(\frac{R_0}{\eta}\right)\varphi\epsilon, \tag{4}$$

where $R_0$ is initial electrical resistance of the sample under the normal conditions, the denominator $\eta = \eta(t) = h(t)/h_0$ takes into account a change of the thickness $h$ of the sample during flat one-dimensional deformation. The rest terms in (4) are the same as in (3). Substitution of the above-obtained model profiles of the temperature $T = T(t)$, the volume $V = V(t)$ and the relative thickness of the sample $\eta = \eta(t)$ provides the model profile of the volume-temperature component of electrical resistance of the shock-compressed sample $R_1 = R_1(t)$:

$$R_1 = \left(\frac{R_0}{\eta(t)}\right)\varphi(t)\epsilon(t). \tag{5}$$

For the experiment discussed herein, the profile $R_1 = R_1(t)$ is shown by the graph *2* in Fig. 4, *a*.

**Table 1.** Coefficients of the model functions for the electro- and thermal-physical properties of tungsten, which are used herein

| $\rho_0$, $\mu\Omega$·cm | $T_0$, K | $V_0$, cm$^3$/mol | $\upsilon_0$, cm$^3$/mol | $n$ | $\alpha$ | $z$ |
|---|---|---|---|---|---|---|
| 5.28 | 293.15 | 9.491 | 28.41 | 48.5(2.7) | 1.2410(5) | 2.9 |

### 4.3. Modeling of the deformation component of the thin tungsten samples under staged-cyclic shock-wave loading

The hydrocode used is also applicable for calculating the deformation characteristics of the sample as a whole. I.e., along with the profiles of the thermodynamic variables, the outcomes of the hydrocode contained, first of all, the above-mentioned time dependence of the relative thickness of the sample as the profile $\eta = h(t)/h_0$. Secondly, in the hydrocode we calculated the strain rate of the sample as $\dot{e} = \dot{e}(t) = (d\eta/dt)/\eta$, its absolute value $|\dot{e}|$ and, finally, the time integral of the absolute value of the strain rate of the sample $|e| = |e(t)| = \int |\dot{e}|d\tau$ within $t_0 < \tau < t$. The profiles $\eta$, $|\dot{e}|$ and $|e|$ for the tungsten sample are designated by the digit *2* in Fig. 3, *b* and the digits *1, 2* in Fig. 4, *b*, respectively.

By having these characteristics, one can formulate the simplest phenomenological model of the deformation component of electrical resistance $R_z$ and then verify it in combination with the experimental profiles $R = R(t)$. Indeed, let us assume that a rate of an increase of electrical resistance of the sample $\dot{R}_z$ is proportional to initial electrical resistance $R_0$ and to the strain rate $e$ of the sample both when it is compressed and unloaded. In other words, let us assume that $\dot{R}_z = zR_0|\dot{e}|$, where $z$ is a free parameter, $|\dot{e}|$ is an absolute strain rate of the sample. In an integral form, this assumption is as follows

$$R_Z = zR_0|e| \tag{6}$$

and, consequently, the summed model profile $R_{mod} = R_{mod}(t)$ of electrical resistance of the sample, which includes the volume-temperature (5) and the deformation (6) component, is calculated by the formula

$$R_{mod} = \left(\frac{R_0}{\eta}\right)\varphi\epsilon + zR_0|e|, \tag{7}$$

where $\eta = \eta(t)$, $\varphi = \varphi(t)$, $\epsilon = \epsilon(t)$, $|e| = |e(t)|$ are output data of the hydrocode, which are in the form of the profiles considered in this section and the previous sections. The graph *3* in Fig. 4, *a* shows the profile $R_{mod} = R_{mod}(t)$ (7), which is calculated with the value $z = 2.9$.

Table 1 shows the full set of the parameters for (7).

In conclusion of this section, we note that it is expedient to use the integral of the absolute strain rate as an optimal characteristic of the deformation component of electrical resistance. Simplified alternative forms for $R_z$ (6), for

example, the dependence on the value of deformation of the strain rate, can be used if we restrict ourselves to variation of electrical resistance of the sample under single shock compression. But, at the same time, in order to match the model and the experimental profiles of electrical resistance during the entire duration of shock compression and subsequent unloading, it is necessary to introduce additional fitting parameters. Therefore, in our case it is more preferable to have the directly proportional dependence (6) of electrical resistance on the integral of the absolute strain rate with one fitting parameter $z$.

We also note that the integral of the absolute strain rate is a nondecreasing positive function. It means that the model relationships (6) and (7) do not allow for annealing or relaxation of defects for the times of the experiment done.

## 5. Discussion of results

Let us consider a relation of the model (3) and the experimental results for the volume-temperature component of specific electrical resistance of tungsten. Above mentioned (Fig. 5) are the temperature $\rho(T)$ and, separately, the volume $\rho(V)$ dependences of $\rho$. In Section 5, the graph *1* in Fig. 6 presents a calculation $\rho_{mod} = \rho_{mod}(V, T)$ of the atmospheric isobar as per (3), which takes into account not only the temperature, but a change of the volume when heating as compared to the experimental $\rho = \rho(V, T)$ atmospheric isobar *2* from the study [11]. As seen, *1* and *2* in Fig. 6 match each other within the temperature range 150−450 K, which includes the temperatures of tungsten in our explosion experiments. The similar result takes place for the isobars at the pressure of 5 GPa as well. Indeed, within the temperature range 150−450 K the model isobar *3* coincides with an experiment *4* from the study [10], which included simultaneous variation of both the temperature and the volume.

Now we address a relation of the experimental profile of electrical resistance of the samples *1* (Fig. 4, *a*) and the model profile *2* of the volume-temperature component of electrical resistance of the shock-compressed samples of tungsten. As seen, already at the first moments of time after $t_0$, when the shock compression pressures do not exceed 3−5 GPa, the experimental electrical resistance *1* significantly exceeds *2*.

However, we note that although further on the experimental electrical resistance that is excessive as compared to $R_1(t)$ increases, nevertheless the profiles *1* and *2* are still qualitatively alike. Based on this, it can be presumed that in addition to the volume-temperature component the experimental profile also has a certain component that smoothly increases in time. It turns out that this component can be the deformation component (6), which together with (5) gives the profile (7). This profile is represented by the graph *3* in Fig. 4, *a*. As seen, the model profile *3* in detail complies with the experimental profile *1* within the time interval $t_0 < t < t_r$, while the pressure in the sample

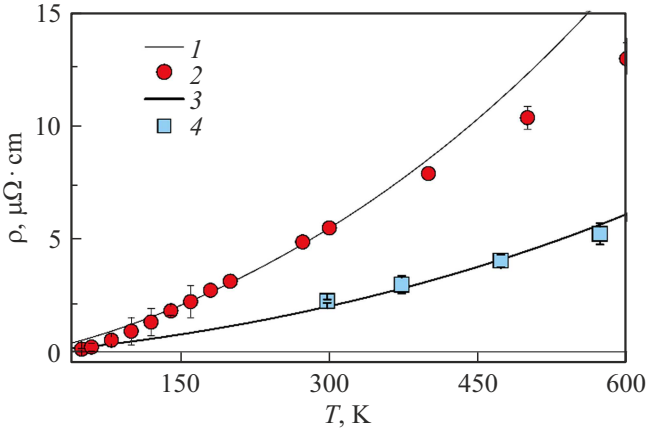


**Figure 6.** Volume-temperature dependence of specific electrical resistance $\rho = \rho(V, T)$. *1* — the model isobar $\rho_{mod} = \rho_{mod}(V, T)$ (3) under the pressure $P = 0$ GPa, *2* — the points of the experimental atmospheric isobar $\rho = \rho(V, T)$ from the study [11], *3* — the model isobar $\rho_{mod}$ (3) when $P = 5$ GPa, *4* — the experimental isobar $\rho$ when $P = 5$ GPa form the study [10].

increases to 15 GPa and then during unloading when $t > t_r$ up to the times $t_p \approx 2.7\,\mu$s, when the pressure decreases to $\approx 3$ GPa.

However, we note that the moment $t_p$ was also worthy of the fact that starting from this moment compliance of the model profile *4* and the experimental profile *1* is sharply violated. This dissonance can be caused both by experimental errors as well as constrainedness of the model. An experimental artefact can be related to application of the two-point recording system that does not take into account a change of electrical resistance of the current conductors. But the electrical resistance profile *4* obtained using the four-point scheme almost coincides with the profile *1* and has the same specific feature at the moment $t_p$ with reaching the plateau $R_p = 0.0283\,\Omega$ at full unloading around $\approx 4\,\mu$s.

The second experimental artefact may be the fact that $R_p$ significantly exceeds electrical resistances $R_{sh}$ of the conserved samples shown in Fig. 2, *b*, *c*. However, this incompliance is reasonably explained by annealing of defects at the high residual temperatures. Indeed, the estimates done demonstrate that under conditions of the shock-wave experiment the surrounding PTFE insulator gets a quite high temperature $\approx 500$ K. During the first minutes after shock-wave impact, the thin tungsten sample will also heat up due to heat exchange with the surrounding insulator.

Thus, most likely, incompliance of the experimental *1* and the model *4* profile of electrical resistance during unloading at the times $t > t_p$ is related to constrainedness of the model (6). The effect can be interpreted as origination of relaxation or annealing of defects after the moment $t_p$. Nevertheless, limiting ourselves to the times $t_0 < t < t_p$, we can say that the represented model of electrical resistance

of the shock-compressed tungsten samples as the sum of the volume-temperature component and the deformation component that is proportional to the integral of the absolute value of the strain rate qualitatively and quantitatively complies with the experiment under the high pressures of staged-cyclic shock compression.

## Conclusion

The study has measured electrical resistances of the shock-compressed tungsten samples at the pressure of up to 15 GPa and the temperatures of up to 360 K.

The volume-temperature dependence of specific electrical resistance of tungsten was reconstructed within the pressure range 0−15 GPa and the temperature range 150−450 K.

It included modeling of the electro-physical properties of tungsten under the conditions of staged-cyclic shock compression.

The deformation component of electrical resistance of the tungsten samples is phenomenologically interpreted by assuming that it has a directly proportional dependence on the integral of the absolute strain rate.

### Funding

The study was done under the State Assignment of the Russian Ministry of Education and Science as per the program „Complex Research of Physical and Chemical Properties and Processes in Matter under Conditions of High-Energy Exposures“, registration No. 124020600049-8.

### Conflict of interest

The authors declare that they have no conflict of interest.

## References

[1] *Elektricheskie yavleniya v udarnykh volnakh*, pod red. V.A. Borisenok, A.M. Molodets, E.Z. Novitskii (Sarov, RFYaTs-VNIIEF, 2005), 265 s. (in Russian).
[2] *Eksperimental'nye metody v fizike udarnykh voln i detonatsii*, pod red. M.V. Zhernokletov (Sarov, FGUP „RFYaTs-VNIIEF“, 2020), 519 s. (in Russian).
[3] B. Gan, J. Li, J. Gao, Q. Zeng, W. Song, Y. Zhuang, Y. Hua, Q. Wu, G. Jiang, Y. Yin, Y. Zhang. Phys. Rev. B, **109**, 115129 (2024). DOI: 10.1103/PhysRevB.109.115129
[4] A.M. Molodets, A.A. Golyshev. FTT, **67** (5), 767 (2025) (in Russian). DOI: 10.61011/FTT.2025.05.60736.75-25
[5] R.A. Graham. *Shock Waves and High-Strain-Rate Phenomena in Metals*, ed. by M.A. Meyers, L.E. Murr (Plenum, NY., 1981), p. 375–386.
[6] A.M. Molodets, A.S. Savinykh, A.A. Golyshev, G.V. Garkushin, G.V. Shilov, A.N. Nekrasov. Fizika metallov i metallovedenie, **123** (5), (in Russian). 554 (2022). DOI: 10.31857/S0015323022050096
[7] A.A. Golyshev, A.M. Molodets. Fizika goreniya i vzryva, (in Russian). **61** (5), 120 (2025). DOI: 10.15372/FGV2024.9467
[8] A.A. Golyshev, V.V. Kim, A.N. Emel'yanov, A.M. Molodets. Prikladnaya mekhanika i tekhnicheskaya fizika, **56** (4), 92 (2015) (in Russian). DOI: 10.15372/PMTF20150409
[9] G.K. White, M.L. Minges. Intern. J. Thermophys., **18** (5), 1269 (1997).
[10] J.A.H. Littleton, R.A. Secco, W. Yong, M. Berrada. J. Appl. Phys., **125**, 135901 (2019). DOI: 10.1063/1.5066103
[11] V.E. Peletskii, E.A. Bel'skaya. *Elektricheskoe soprotivlenie tugoplavkikh metallov*, spravochnik red. red. L.E. Sheindlina (Energoatomizdat, M., 1981), 96 s. (in Russian).

*Translated by M.Shevelev*

## Appendix

### Thermal equation of state of tungsten

The thermal equation of state used herein (the dependence of pressure $P = P(V, T)$ on the specific volume $V$ and the temperature $T$) for tungsten from the study [8] is written as

$$P = 3R\Theta\frac{\gamma}{V}\left(\frac{1}{2} + \frac{1}{\exp(\Theta/T) - 1}\right) + P_x, \qquad \text{(A1)}$$

where $R$ is the specific gas constant, the key functions $\Theta = \Theta(V)$, $\gamma = \gamma(V)$ and $P_x = P_x(V)$ are algebraic volume functions. So, the characteristic temperature $\Theta = \Theta(V)$ is expressed as

$$\Theta = \Theta_0\left(\frac{\upsilon_0 - V}{\upsilon_0 - V_0}\right)^2\left(\frac{V_0}{V}\right)^{2/3}, \qquad \text{(A2)}$$

$$\upsilon_0 = V_0\left(1 + \frac{2}{\gamma_0 - 2/3}\right). \qquad \text{(A3)}$$

In (A2) the parameter $\Theta_0$ is an initial value of the characteristic temperature $\Theta_0 = \Theta(V_0)$ at the initial specific volume $V_0$, at the initial room temperature $T_0 = 298.15$ K and the initial atmospheric pressure. The parameter $\upsilon_0$ is expressed via $V_0$ and the Gruneisen thermodynamic parameter $\gamma_0 = \gamma_0(V_0, T_0)$. The volume dependence of the Gruneisen coefficient $\gamma = \gamma(V)$ and the potential pressure $P_x = P_x(V)$ is written as

$$\gamma = -\frac{d\ln\Theta}{d\ln V} = \frac{2}{3} + \frac{2V}{\upsilon_0 - V}, \qquad \text{(A4)}$$

$$P_x = 3C_1x^{1/3}\left(-\frac{1}{5}x^{-2} + 2x^{-1} + 6 - x + \frac{1}{7}x^2\right) + C_2. \qquad \text{(A5)}$$

$$x = V/\upsilon_x. \qquad \text{(A6)}$$

**Table 2.** Parameters of the thermal equation of state (A1) for tungsten

| $\Theta_0$, K | $V_0$, cm$^3$/mol | $\upsilon_0$, cm$^3$/mol | $\upsilon_x$, cm$^3$/mol | $C_1$, GPa | $C_2$, GPa |
|---|---|---|---|---|---|
| 287.25 | 9.491 | 28.41 | 26.801 | −313.876 | 6471.738 |

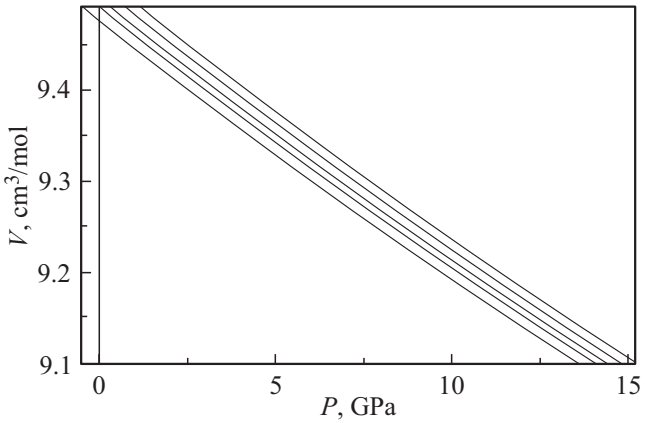


**Figure 7.** Isotherms of tungsten (A1) at the temperatures (from bottom to top) 173, 298, 373, 473, 573 K.

The set of the defining parameters $\Theta_0, V_0, \upsilon_0, \upsilon_x, C_1, C_2$ for (A1)–(A6) and their numerical values from the study [8] are given in Table 2. Fig. 7 shows some isotherms (A1) for tungsten, which are used when recalculating the values of $\rho(P, T)$ into $\rho(V(P), T)$.